Proceedings of the Seventh International Conference on
Railway Technology: Research, Development and Maintenance
Edited by: J. Pombo
Civil-Comp Conferences, Volume 15, Paper 11.18
Civil-Comp Press, Edinburgh, United Kingdom, 2026
ISSN: 2753-3239, doi: 10.4203/ccc.15.11.18


# Target Guidance Gap Reconstruction and Control Optimization for High-Speed Maglev Horizontal Curves

**Y. Zhang[1], J. Xu[1], H. Li[2], D. Gao[1], W. Ji[1] and W. Wang[1]**

**[1]College of Transportation, Tongji University, Shanghai, China**
**[2]Railway Science & Technology Research & Development Center, China Academy of Railway Sciences Corporation Limited, Beijing, China**

## Abstract

To address the guidance reference distortion caused by the discrete straight-line approximation of track girders in horizontal curve sections, this paper proposes a target guidance gap reconstruction and control optimization method for high-speed maglev. First, a multi-parameter constrained reconstruction model is established, taking the circular curve radius and the front and rear inward offsets as the core variables. Under various constraint conditions, a smooth reference alignment highly consistent with actual track characteristics is iteratively fitted. Subsequently, the lateral deviation of the reconstructed alignment is superimposed on the theoretical gap to generate the target guidance gap, which is then incorporated into the PID control system to mitigate the disturbances caused by the discrete straight-line of track girders in horizontal curve sections. Finally, the effectiveness of the proposed method is verified based on data of the Shanghai Maglev Line. The results indicate that the fluctuation range of the optimized guidance gap narrows from 5–15 mm to 8–13 mm, and the peak lateral vibration acceleration of the car body decreases from 1.3 m/s² to 0.57 m/s². The proposed method significantly improves the running stability and ride comfort of high-speed maglev vehicles negotiating horizontal curves.

**Keywords:** high-speed maglev, guidance gap, guideway surface, control optimization, ride comfort, alignment reconstruction.

## 1 Introduction

High-speed maglev transportation as an advanced rail transit mode, especially as it moves towards a 600 km/h operating environment, imposes extremely stringent requirements on the smoothness of the track functional surface and guidance accuracy [1,2]. Compared with traditional wheel-rail systems, maglev vehicles rely on non-contact electromagnetic forces to achieve levitation and guidance. Minute irregularities can not only induce vehicle-guideway coupled vibrations but also directly affect the levitation and guidance stability, as well as the operational safety of the system [3]. In practical engineering construction, due to technological and structural limitations, horizontal curve sections of high-speed maglev track girders are typically arranged using a discrete straight-line approximation method [4,5]. This alignment deviation results in the guideway guidance surface not being a continuously smooth horizontal curve, but rather a series of minute broken-line segments.

The core of the guidance control system lies in achieving stable operation through real-time adjustments of the gap between the vehicle and the guidance surface. Currently, extensive research has been conducted on maglev control algorithms and track condition characterization methods. Ji et al. [6,7] comprehensively explored fault-tolerant control methods utilizing adaptive fuzzy controllers and multi-model mechanisms to handle actuator failures and parameter uncertainties; Zhang et al. [8-10] established prediction models and feature characterization systems for high-speed maglev track irregularities. However, when the vehicle negotiates horizontal curve sections, existing guidance control methods generally adopt the rated guidance gap directly as the control reference [11,12], causing the actual running trajectory of the train to match the functional surface of the track girders characterized by the discrete straight-line approximation.

The key to resolving this core issue lies in constructing a continuous horizontal curve alignment that conforms to the actual deformation feature of the guidance surface, and thereby correcting the target guidance gap to provide a smooth reference baseline for train operation. However, existing alignment fitting methods [13-15] mostly originate from conventional railways and present obvious limitations when applied to high-speed maglev. On the one hand, they fail to integrate the design specification requirements unique to maglev engineering; on the other hand, they lack sufficient consideration of the tolerance of the guidance gap.

This paper proposes a target guidance gap reconstruction and control optimization method for high-speed maglev horizontal curves. Based on the measurement data of the track girder guidance surface, this method iteratively fits an ideal horizontal curve conforming to the actual characteristics of the track girders, following the engineering specifications and guidance gap limits. The geometric deviations are mapped to the target guidance gap to provide a basis for optimizing controller signals, thereby improving the running quality of the train passing through horizontal curves.

## 2 Analysis of spatial deformation characteristics of guidance surfaces in high-speed maglev functional components

### 2.1 Analysis of Guidance Reference Distortion of Track Girders

When high-speed maglev vehicles negotiate horizontal curve sections, their running stability is closely related to the control accuracy of the guidance gap. Under ideal conditions, the vehicle needs to run along a continuous and smooth horizontal curve trajectory, and the guidance control system achieves stable guidance force output by adjusting the gap between the vehicle and the guideway guidance surface in real time.

However, constrained by construction technology requirements and the limitations of the track structure, the track girders in horizontal curve sections of high-speed maglev are typically arranged using a discrete straight-line approximation method in practical engineering. This manufacturing and installation process results in the actual constructed guideway guidance surface not being an ideal, continuously smooth horizontal curve, but rather being composed of a series of discrete minute broken-line segments spliced together, as shown in Figure 1.

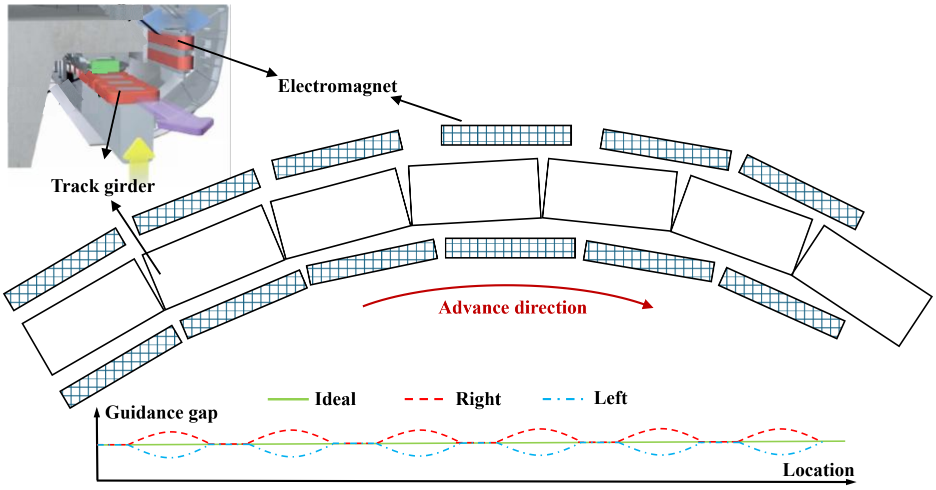


Figure 1: High-speed maglev horizontal curve characteristic and guidance gap

If the control system directly uses the broken-line guidance surface of the actual track girders as the spatial reference, the measured guidance gap obtained by sensors cannot accurately reflect the true relative positional relationship required for the vehicle to run smoothly along the ideal smooth curve. This will cause the vehicle's guidance control system to continuously track distorted targets that do not match the ideal smooth trajectory when passing through curves. As illustrated by the red and blue dashed lines in Figure 1, the guidance gap fluctuates at the girder joint positions, which restricts further improvements in the curve negotiation performance and ride comfort of the vehicle.

## 2.2 Guidance surface feature extraction based on spatial coordinates

To overcome the track geometric reference error, the primary task is to accurately obtain the spatial position characteristics of the actual track girder guidance surface. A mathematical model of the discrete characteristics of the guidance surface is constructed based on measured data. First, the discrete spatial coordinate measurement data based on the construction coordinate system of the high-speed maglev track girder are obtained. Let the measured data set of the guidance surface containing $N$ measurement points be defined as $\mathbf{P}$, where the $i$th measurement coordinate point can be expressed as a two-dimensional planar vector:

$$\mathbf{P}_i = \left(X_i, Y_i\right), \quad i \in \{1,2,3,\ldots,N\} \tag{1}$$

where, $X_i$ is the east coordinate of the $i$th point, and $Y_i$ is the north coordinate of the $i$th point. This data set **P** will serve as the high-precision original input data for subsequent alignment identification and continuous curve reconstruction.

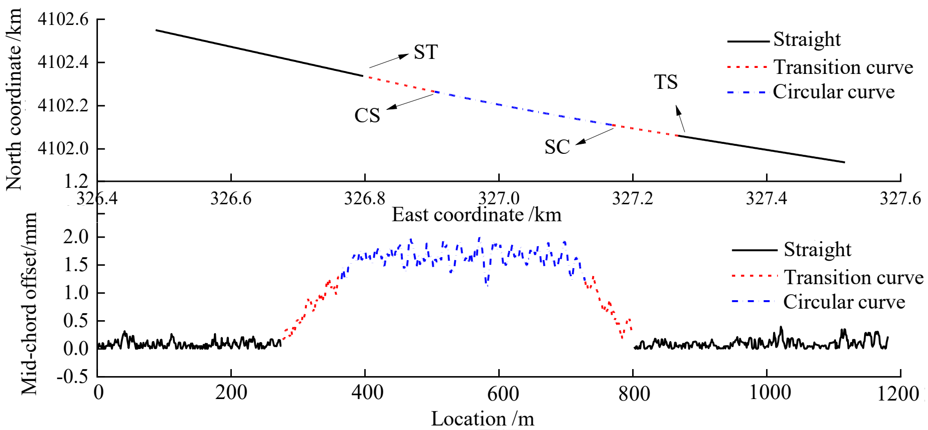

Figure 2: Identification of guidance surface alignment elements

After obtaining the discrete measurement data, it is necessary to identify the initial positions of the Tangent-to-Spiral (TS), Spiral-to-Curve (SC), Curve-to-Spiral (CS), and Spiral-to-Tangent (ST) points. The mid-chord offset [16, 17] is introduced for the classification of the alignment. Three equally spaced coordinate points—the $i$-$n_w$ point, the $i$th point, and the $i$+$n_w$ point—are selected from **P**, where $n_w$ is the set sampling interval window width for the measurement points. Calculate the normal distance between the $i$th point and the reference chord, i.e., the mid-chord offset $v_i$:

$$v_i = \left| \left( Y_i - Y_{i-n_w} \right) \cos \alpha_i - \left( X_i - X_{i-n_w} \right) \sin \alpha_i \right| \qquad \alpha_i = \arctan \left( \frac{Y_{i+n_w} - Y_{i-n_w}}{X_{i+n_w} - X_{i-n_w}} \right) \tag{2}$$

By calculating the mid-chord offset $v_i$ using a sliding window for all measurement points along the entire line, the positions of the alignment element boundary points on the guidance surface can be determined based on the following rules:

(1) Tangent zone: When the measurement points are located in a tangent, the mid-chord offset fluctuates slightly around 0 due to measurement noise.

(2) Circular curve zone: When the measurement points are located in a circular curve, the mid-chord offset $v_i$ fluctuates around a non-zero constant $C$ ($C \neq 0$).

(3) Boundary transition point: Along the direction of advancing mileage, when the fluctuation trend of the mid-chord offset $v_i$ undergoes a significant sudden change, the corresponding measurement point position is determined as the approximate position of the alignment boundary point.

Relying on this strategy, the unordered measurement data are divided into tangent, transition curve, and circular curve sections. The mid-chord offsets calculated using the measured data are shown in Figure 2. Combined with the aforementioned judgment strategy, the various alignment elements of the guidance surface line can be clearly distinguished.

# 3 Multi-parameter constrained alignment reconstruction model for guidance gap optimization

Based on the preliminary positioning of the alignment elements of the track girder guidance surface, a continuous, smooth virtual control reference that meets the gap requirements is constructed to eliminate the geometric reference error caused by the "discrete straight-line approximation curve."

After obtaining the initial mileages of the TS, SC, CS, and ST points, the spatial measurement data of the guidance surface are accurately divided into different alignment element sections, including the front tangent section, front transition curve section, circular curve section, rear transition curve section, and rear tangent section. First, the orthogonal least squares method [18] is used to fit the measurement coordinate points within the front and rear tangent sections, respectively, to obtain the fitted straight-line equations. Subsequently, the intersection coordinates ($X_{\mathrm{JD}}$, $Y_{\mathrm{JD}}$) and the deflection angle $\alpha$ of the two straight lines are calculated, as shown in Figure 3.

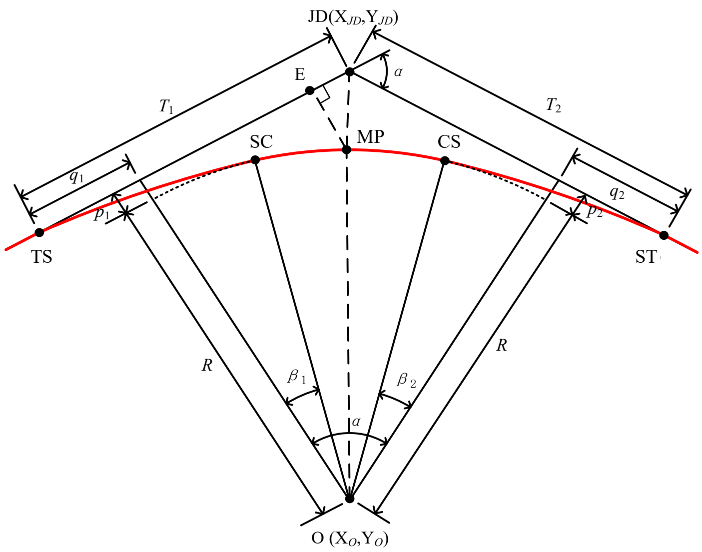

Figure 3. Horizontal alignment and related parameters

To ensure that the reconstructed alignment can maximally fit the actual broken-line track girders, an optimization model is established in this paper with the core objective of minimizing the sum of squared deviations between the measurement points and the circular curve. Considering the geometric characteristics of maglev alignment design, the objective function is transformed into a mathematical expression controlled solely by three core variables: the front inward offset $p_1$, the rear inward offset $p_2$, and the fitted circular curve radius $R$:

$$\begin{aligned} & f(p_1, p_2, R) \\ & = \min \sum_{i=1}^{n_Y} \left[ (X_i - X_{\mathrm{O}})^2 + (Y_i - Y_{\mathrm{O}})^2 - R^2 \right] \\ & = \min \sum_{i=1}^{n_Y} \left[ (X_i - X_{\mathrm{MP}} - R \cdot \cos\alpha_{\mathrm{MP-O}})^2 + (Y_i - Y_{\mathrm{MP}} + R \cdot \sin\alpha_{\mathrm{MP-O}})^2 - R^2 \right] \end{aligned} \tag{3}$$

where, $n_{\mathrm{c}}$ is the number of coordinate points contained within the circular curve section; ($X_i$, $Y_i$) is the coordinates of the $i$-th point within the circular curve; ($X_O$, $Y_O$) is the center coordinates of the fitted circle. ($X_O$, $Y_O$) can be derived through analytical geometric relations by combining the midpoint coordinates of the curve ($X_{MP}$, $Y_{MP}$) and the azimuth angle $\alpha_{QZ}$, while introducing constant parameters such as the intersection coordinates ($X_{JD}$, $Y_{JD}$), tangent lengths, tangent offsets, and transition curve tangent angles. In this objective function, the equations of the front and rear tangent sections are fixed, and the intersection parameters and azimuth angles are constants. Only $p_1$, $p_2$, and $R$ are used as optimization variables.

$$X_{\mathrm{MP}} = X_{\mathrm{JD}} + \cos\left[\alpha_{\text{JD-TS}} + \arctan\left(\frac{2R+2p_1-R\cos\phi}{2T_1-2q_1-R\sin\phi}\right)\right] \cdot \sqrt{(R+p_1)^2+(T_1-q_1)^2+\frac{R^2}{4}+(p_1R-\frac{R}{2})\cos\phi+(q_1R-T_1R)\sin\phi} \tag{4}$$

$$Y_{\mathrm{MP}} = Y_{\mathrm{JD}} + \sin\left[\alpha_{\text{JD-TS}} + \arctan\left(\frac{2R+2p_1-R\cos\phi}{2T_1-2q_1-R\sin\phi}\right)\right] \cdot \sqrt{(R+p_1)^2+(T_1-q_1)^2+\frac{R^2}{4}+(p_1R-\frac{R}{2})\cos\phi+(q_1R-T_1R)\sin\phi} \tag{5}$$

In equations (4) to (7), the intersection coordinate, the front and rear tangent length ($T_1$, $T_2$), the front and rear tangent offset ($q_1$, $q_2$), the azimuth angle $\alpha_{\text{TS-JD}}$, the front and rear transition curve tangent angle ($\beta_1$,$\beta_2$), and deflection angle $\alpha$ are all constants. Only the front and rear inward offsets ($p_1$, $p_2$) and the fitted circular curve radius $R$ are variables, where $\phi=\alpha-\beta_1+\beta_2$.

The stringent safety requirements of high-speed maglev systems dictate that the reconstructed alignment must simultaneously satisfy design specifications and the physical limits of the electromagnets. Therefore, when solving the aforementioned objective function, multiple constraint conditions must be introduced:

(1) Minimum circular curve radius constraint: This ensures that the centrifugal acceleration and lateral stability of the vehicle under maximum speed conditions do not exceed permissible limits, i.e., $R > R_{\min}$.

(2) Minimum transition curve length constraint: This ensures that the rate of change of curvature in the curve transition section remains within a safe range. The constraint conditions satisfied by the front and rear transition curve lengths $l_{s,1}$ and $l_{s,2}$ are as follows, where $l_{s,\min}$ represents the minimum transition curve length.

$$\begin{cases} l_{s1} \geq l_{s,\min} \\ l_{s2} \geq l_{s,\min} \end{cases} \xrightarrow{l_{s1}=\sqrt{24R\times p_1}} \begin{cases} p_1 \geq l_{s,\min}^2 / 24R \\ p_2 \geq l_{s,\min}^2 / 24R \end{cases} \tag{8}$$

(3) Minimum circular curve length constraint:

$$\begin{gathered} R\cdot\alpha - \frac{(l_{s1}+l_{s2})}{2} \geq L_{\min} \\ \Rightarrow p_1 + p_2 \leq \frac{(R\cdot\alpha - L_{\min})^2}{6R} \end{gathered} \tag{9}$$

(4) Maximum guidance gap constraint: To prevent the vehicle from experiencing mechanical collisions with the guideway or loss of control, it must be ensured that the maximum deviation between the reconstructed alignment and the actual guidance surface does not exceed the maximum permissible guidance gap limit $G_{\max}$.

$$R - \sqrt{\left(X_i - X_{\mathrm{QZ}} - R\cdot\cos\alpha_{\text{QZ-O}}\right)^2 + \left(Y_i - Y_{\mathrm{QZ}} + R\cdot\sin\alpha_{\text{QZ-O}}\right)^2} \leq G_{\max} \tag{10}$$

After establishing the objective function and the four major constraint conditions above, a three-variable nonlinear programming algorithm is employed to solve the model. Through optimization calculations, the optimal combination coefficients ($p_1$, $p_2$, $R$) are obtained, from which the design parameters of the reconstructed alignment satisfying all control limits are subsequently derived.

Since the initial extraction of the boundary point mileages relies on a rough estimation of the mid-chord offset, local deviations are inevitable. Upon obtaining the optimal parameters from the nonlinear programming solver, the position coordinates of the TS, SC, CS, and ST points are updated using the following method:

$$\begin{cases} M_{\mathrm{TS}} = M_{\mathrm{start}} + \sqrt{\left(X_{\mathrm{TS}} - X_{\mathrm{start}}\right)^2 + \left(Y_{\mathrm{TS}} - Y_{\mathrm{start}}\right)^2} \\ M_{\mathrm{SC}} = M_{\mathrm{TS}} + l_{s1} \\ M_{\mathrm{CS}} = M_{\mathrm{SC}} + \left(L - l_{s1} - l_{s2}\right) \\ M_{\mathrm{ST}} = M_{\mathrm{CS}} + l_{s2} \end{cases} \tag{11}$$

where, $M_{\mathrm{start}}$ is the starting mileage; $M_{\mathrm{TS}}$, $M_{\mathrm{SC}}$, $M_{\mathrm{CS}}$, and $M_{\mathrm{ST}}$ represent the mileages of the TS, SC, CS, and ST points, respectively. $X_{\mathrm{TS}}$, $Y_{\mathrm{TS}}$ are the east and north coordinates of the TS point; $X_{\mathrm{start}}$, $Y_{\mathrm{start}}$ are the coordinates of the starting point; and $L$ is the length of the circular curve.

The updated boundary point position serves as the input for the subsequent iteration, which triggers a re-division of the alignment elements and a subsequent re-execution of the multi-parameter constrained model solver. A stability convergence criterion is established: when the mileage difference for the same boundary point calculated in two consecutive iterations is smaller than a predefined threshold, the model is considered to have converged. The resulting output parameters are the final design parameters for the reconstructed alignment of the guidance surface, which are fully adapted to the actual track girders.

### 3.3 Mapping from geometric deviation to target guidance gap

Based on the reconstructed alignment of the guidance surface determined by the final design parameters, the lateral deviation between the measurement data and the reconstructed alignment is calculated. By taking the rated guidance gap into account, the target guidance gap matching the actual deformation of the track girder can be obtained.

After determining the final design parameters, a continuous, smooth reconstructed alignment of the guidance surface that conforms to reality can be generated. Subsequently, the lateral deviation $\Delta h$ of each measurement point relative to this reconstructed alignment is calculated. Along the direction of advancing mileage, when the measurement point is located on the left side of the line, the lateral deviation $\Delta h$ takes a negative sign; when on the right side, it takes a positive sign. The specific calculation method for $\Delta h$ is as follows:

(1) For tangent: The standard point-to-line distance formula is used to directly calculate the lateral deviation.

(2) For circular curve: The lateral deviation is the distance from the measurement point to the fitted circle center minus the fitted radius:

$$\Delta h_i = \sqrt{(X_i - X_O)^2 + (Y_i - Y_O)^2} - R \tag{12}$$

(3) For transition curve: The measurement coordinates are transformed from the global coordinate system of the track girder to the independent coordinate system of the transition curve. Using the TS/ST point as the starting point, the corresponding coordinate point on the curve is found along the direction perpendicular to the tangent of the transition curve. The Euclidean distance between the two points is then calculated and taken as the lateral deviation of that measurement point. Taking the front transition curve as an example, the corresponding point of the measurement coordinate point on the transition curve is:

$$\begin{cases} x'_{1,i} = l_i - \dfrac{l_i^5}{40R^2 l_1^2} + \dfrac{l_i^9}{3456R^4 l_1^4} \\ y'_{1,i} = \dfrac{l_i^3}{6Rl_1} - \dfrac{l_i^7}{336R^3 l_1^3} \end{cases} \tag{13}$$

where, $x'_{1,i}$, $y'_{1,i}$ represent the abscissa and ordinate of the corresponding point for the measurement point $i$ in the independent coordinate system of the transition curve; $l_1$ represents the total length of the transition curve, and $l_i$ is the curve length from the corresponding point of measurement point $i$ on the transition curve to the TS/ST point.

Finally, the theoretical guidance gap $G_{h,i}$ originally adopted by the control system is superimposed with the calculated lateral deviation $\Delta h$ to generate the reconstructed target guidance gap $G'_{h,i}$.

$$G'_{h,i} = G_{h,i} - d_i \tag{14}$$

Adopting the $G'_{h,i}$ as the control reference can reflect the positional relationship required for the vehicle to run along the ideal smooth curve, thereby eliminating the geometric deviation disturbances caused by the "discrete straight-line approximation curve." The relationship among the reconstructed alignment of the guidance surface, the track girder, and the guidance electromagnet is illustrated in Figure 5.

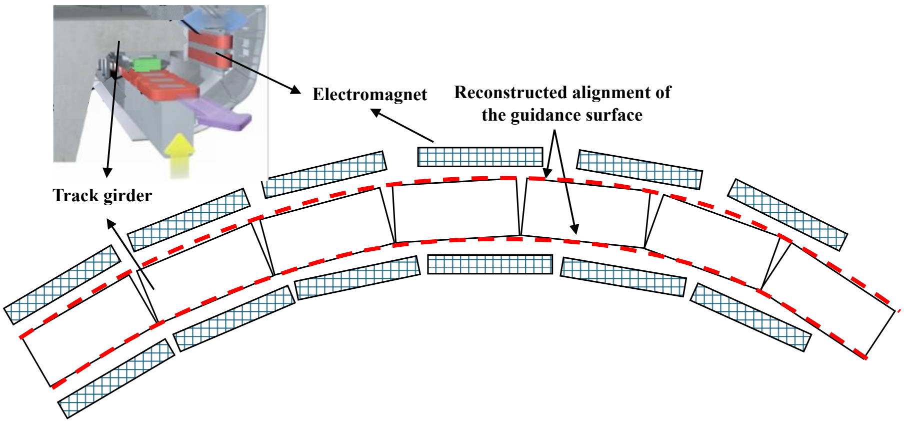

Figure 5: Reconstructed alignment, track girder, and electromagnet

The calculated target guidance gap $G'_{h,i}$ at each point is adopted as the new tracking target value for the guidance control system. In the control loop, sensors collect the measured guidance gap data $g(t)$ of the vehicle at time $t$ in real time. The control system calculates the control deviation between this measured sensor value and the target guidance gap at the corresponding position, and employs a PID control law [19, 20] to calculate the controller output command $u(t)$—namely, the optimized controller signal. This ultimately achieves stable operation control of the maglev vehicle when passing through horizontal curves. The calculation is expressed as Equation (15):

$$u(t) = K_p\left(g(t) - G'_{h,i}\right) + K_i\int_0^t\left(g(t) - G'_{h,i}\right)d\tau + K_d\frac{d\left(g(t) - G'_{h,i}\right)}{dt} \tag{15}$$

where, $K_p$, $K_i$, and $K_d$ are the proportional, integral, and derivative coefficients of the guidance controller, respectively.

# 4 Implementation effectiveness and guidance control optimization verification

## 4.1 Simulation model and operating conditions

To quantitatively evaluate the implementation effectiveness of the aforementioned control optimization scheme, a vehicle-guideway dynamics co-simulation platform for high-speed maglev was constructed in this paper based on multi-body dynamics software and control system simulation software.

(1) Vehicle subsystem: A multi-rigid-body model containing components such as the car body, levitation bogies, and electromagnets is established. The components are connected to each other through secondary suspensions and articulated structures.

(2) Guideway subsystem: The alignment parameters of the horizontal curve section are set, including tangent, circular curve, and transition curve sections. According to the actual engineering, the circular curve section in the model adopts track girders formed by splicing multiple standard-length straight girders end-to-end, so as to simulate the true spatial state of the "discrete straight-line approximation curve."

(3) Controller parameter setting: The guidance control module is configured with a control group using the traditional guidance gap as the tracking target, and an optimization group using the reconstructed target guidance gap proposed in this paper as the tracking target. The PID parameters ($K_p$, $K_i$, $K_d$) for both groups are kept identical to exclude the interference of parameter tuning on the verification results.

## 4.2 Comparative analysis of vehicle dynamic responses

Shanghai Maglev Line is the world's only high-speed maglev in commercial operation. The total length is approximately 30 km, with a maximum operating speed of 430 km/h, and the overview of the entire line is shown in Figure 6.

Simulation analysis is conducted on one of the horizontal curves in this line. The vehicle passes through the horizontal curve section at a constant set speed of 430 km/h. System response data under two conditions—the traditional constant target guidance gap and the reconstructed target guidance gap—are extracted for comparison.

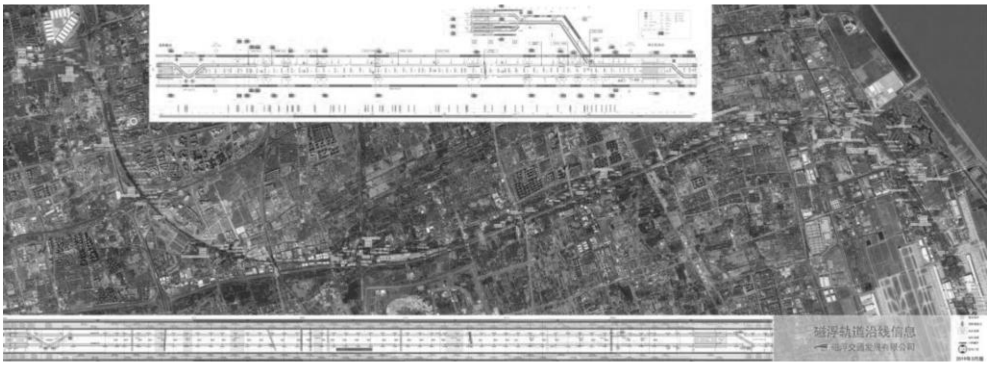

Figure 6: Shanghai Maglev Line

(1) Analysis of the guidance gap fluctuation

The train running stability simulated and calculated using the two-target guidance gap control strategies is shown in Figure 7. Under the traditional control strategy, due to geometric interference of the actual track girder "broken line" reference, the actual guidance gap measured by the sensor fluctuates within the range of 5–15 mm. After introducing the reconstructed target guidance gap, the controller tracks a smooth reference that is compatible with the track feature. The fluctuation amplitude of the output commands is reduced, distributing within 8–13 mm. This not only enhances the operational stability of the train but also reduces unnecessary power consumption of the electromagnet coils, thereby extending the service life of the actuators.

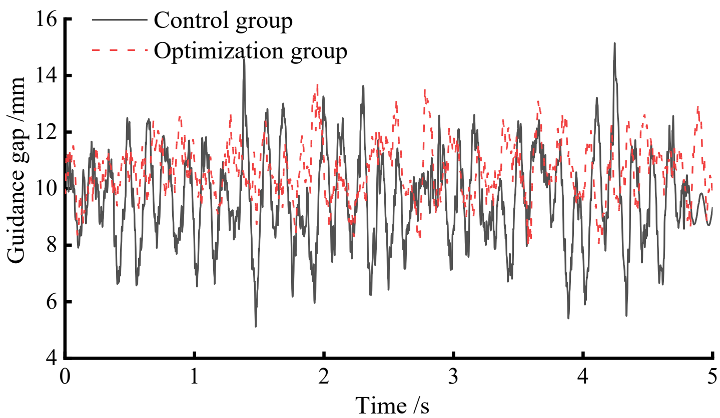


Figure 7: Guidance gap fluctuation

**(2) Evaluation of vehicle dynamic response**

The lateral vibration acceleration of the car body as the vehicle negotiates the horizontal curve is extracted for signal waveform analysis. Figure 8 indicates that when the vehicle in the optimization group passes through the curve section, the peak lateral acceleration of its car body decreases from 1.3 m/s² to 0.57 m/s², which is a 56% reduction compared to the control group, demonstrating a marked improvement in ride comfort.

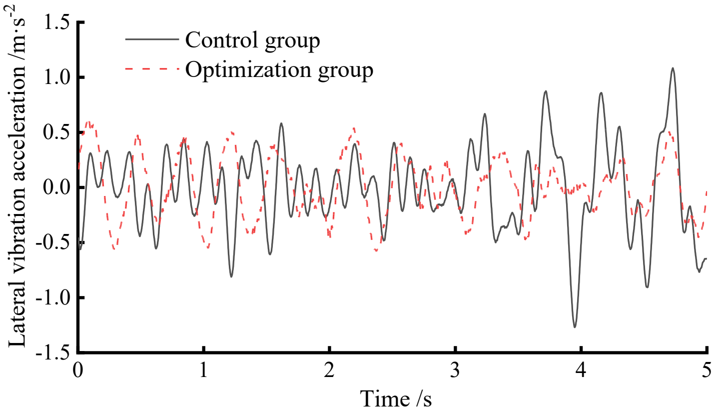

Figure 8: Lateral vibration acceleration of the car body

In summary, the target guidance gap reconstruction method proposed in this study can significantly improve the running stability and ride comfort of high-speed maglev vehicles passing through horizontal curves, fully compensating for the control deficiencies caused by the "discrete straight-line approximation curve" of the track girders. This verifies that the method proposed in this study is of significant value for enhancing the running performance of high-speed maglev systems.

## 5 Conclusions and Contributions

(1) The sources of guidance reference distortion are analyzed, and the iterative fitting and reconstruction of the horizontal curve alignment are achieved. By incorporating the mid-chord offset to identify the alignment boundary points of the guidance surface, a multi-parameter constrained reconstruction model has established, taking the circular curve radius and the front and rear inward offsets as core variables. Under constraints such as the minimum curve radius, transition curve length, and maximum guidance gap, this model constructed a smooth reference alignment that highly conforms to the actual feature of the track girders.

(2) The traditional control strategy of adopting a constant theoretical guidance gap as the tracking target was abandoned. By calculating the lateral deviation of the measurement points relative to the reconstructed alignment and superimposing it on the theoretical guidance gap, a brand-new target guidance gap was generated. Introducing this into the PID guidance control loop effectively shielded the high-frequency disturbances at girder joints and discrete angles, compensating for the running trajectory irregularity defects caused by the "discrete straight-line approximation curve" of the track girders.

(3) Verification results based on the 430 km/h operating conditions of the Shanghai Maglev Demonstration Line indicate that after optimizing the target guidance gap, the gap fluctuation range narrowed from 5–15 mm under the traditional control strategy to 8–13 mm, and the peak lateral vibration acceleration of the car body decreased from 1.3 m/s² to 0.57 m/s². The proposed method improves the matching between the guidance control target and the ideal running trajectory, enhancing the running stability of high-speed maglev vehicles passing through horizontal curves.

## Acknowledgements

This work was supported by the National Natural Science Foundation of China (52232013, 52332011), the National Key Research and Development Program of China (2023YFB4302502).

# References

[1] Chen C, Xu J, Yang J, et al. (2025). Dynamic analysis of high-speed maglev magnetic coupling and experimental study on vehicle-bridge characteristics. *Journal of Vibration and Control*, DOI: 10.1177/10775463251377125

[2] Ji W, Lin X, Sun Y, et al. (2025). Intelligent Fault-tolerant control for high-speed maglev transportation based on error-driven adaptive fuzzy online compensator. *IEEE Transactions on Intelligent Transportation Systems*, *26*(10): 17814-17823.

[3] Wang W, Song Y, Xu J, et al. (2025). Track Irregularity Prediction and Effect on the Dynamic Response of the 600 km/h Maglev System. *IEEE Transactions on Vehicular Technology*. DOI: 10.1109/TVT.2025.3595644

[4] Deng Y, Wei Q, Ni Y, et al. (2007). Research on fitting techniques of guideway in high-speed maglev TR system. *Journal of Beijing Jiaotong University*, 31(4): 96-100.

[5] Wang Z, Xu Y, Li G, et al. (2020). Optimization of horizontally curved track in the alignment design of a high-speed maglev line. *Structure and Infrastructure Engineering*, 16(7), 1019-1036.

[6] Ji W, Lv D, Luo S, et al. (2024). Multiple models-based fault tolerant control of levitation module of maglev vehicles against partial actuator failures. *IEEE Transactions on Vehicular Technology*, 74(2), 2231-2240.

[7] Sun Y, Li F, Ji W, et al. (2025). Robust control for suspension system of maglev train considering parametric uncertainty and unidirectional input constraint. *IEEE Transactions on Industry Applications*. 61(6): 9671 – 9680.

[8] Zhang Y, Xu J, Wang W, et al. (2026). Model-driven intelligent graded evaluation of high-speed maglev track irregularity and its application validation. *Journal of Vibration and Control*, DOI: 10.1177/10775463261427793

[9] Wang W, Xu J, Chen C, et al. (2025). Track irregularity in high-speed maglev systems based on line technical standards and its applications. *Journal of the China Railway Society*, 47(7): 214-224. in Chinese

[10] Xu J, Chen Z, Zheng Q, et al. (2025). Data-driven modeling of high-speed maglev track irregularity. *Probabilistic Engineering Mechanics*, 103798. DOI: 10.1016/j.probengmech.2025.103798

[11] Shi J, Fang W, Wang Y, et al. (2014). Measurements and analysis of track irregularities on high speed maglev lines. *Journal of Zhejiang University SCIENCE A*, 15(6): 385-394.

[12] Li B, Zhao C, Li X, et al. (2020). Dynamics modeling analysis and experiment of the guidance control system of high-speed maglev train. *IEEE Access*, 8: 206207-206221.

[13] Zhang Y, Shi J, Tan S, et al. (2025). A smoothness control method for kilometer-span railway bridges with analysis of track characteristics. *Computer-Aided Civil and Infrastructure Engineering*, 40(2): 215-242.

[14] Zhang Y, Shi J, Tan S, et al. (2025). Optimizing maintenance of vertical curves in high-speed railways. *Automation in Construction*, 2023, 152: 104947.

[15] Zhang Y, Shi J, J.N.Varandas, et al. (2025). An interval prediction system for track irregularity after tamping based on multi-module machine learning and pointwise scaling approach. *Computer-Aided Civil and Infrastructure Engineering*, 40(27): 4797-4823.

[16] Zhang Y, Shi J, Xiao J, et al. (2025). An adaptive multi-factor correction method for tamping adjustment with fulfilment rate characteristic analysis. International Journal of Rail Transportation, 2025: 1-32.
[17] Zong L, Hu J, Pan M, et al. (2025). Experimental measurement of track irregularities in EMS maglev systems using the mid-chord offset method and inverse filtering technology. *Proceedings of the Institution of Mechanical Engineers, Part F: Journal of Rail and Rapid Transit*, 239(2): 106-115.
[18] Shi J, Zhang Y, Chen Y, et al. (2023). A smoothness optimization method for horizontal alignment considering ballasted track maintenance. *Computer-Aided Civil and Infrastructure Engineering*, 38(6): 739-761.
[19] Chen C, Xu J, Lin G, et al. (2022). Model identification and nonlinear adaptive control of suspension system of high-speed maglev train. *Vehicle System Dynamics*, 60(3): 884-905.
[20] Li H, Zhang W, Hong Y, et al. Research on influence of eddy current effects between rails and electromagnets in maglev vehicles under nonuniform magnetic fields, *IEEE Transactions on Instrumentation and Measurement*, 2026, DOI: 10.1109/TIM.2025.3650248